In situ gene expression profiling of the thermoacidophilic alga C *yanidioschyzon* in relation to visible and ultraviolet irradiance

Authors: Dana J. Skorupa, Richard W. Castenholz, Aurélien Mazurie, Charles Carey, Frank Rosenzweig, & Timothy R. McDermott

Skorupa DJ, Castenholz RW, Mazurie A, Carey C, Rosenzweig F, McDermott TR, "In situ gene expression profiling of the thermoacidophilic alga Cyanidioschyzon in relation to visible and ultraviolet irradiance," Environmental Microbiology, June 2014 16(6): 1627–1641.

In situ gene expression profiling of the thermoacidophilic alga *Cyanidioschyzon* in relation to visible and ultraviolet irradiance

Dana J. Skorupa,[1] Richard W. Castenholz,[4] Aurélien Mazurie,[2] Charles Carey,[2] Frank Rosenzweig[5] and Timothy R. McDermott[3]*

[1]*Department of Microbiology,*

[2]*Bioinformatics Core and*

[3]*Department of Land Resources and Environmental Sciences, Montana State University, Bozeman, MT, 59717, USA.*

[4]*Institute of Ecology and Evolution, University of Oregon, Eugene, OR, 97403-5289, USA.*

[5]*College of Arts and Sciences, University of Montana, Missoula, MT 59812, USA.*

Summary

Ultraviolet and high-intensity visible radiation gener-ate reactive intermediates that damage phototrophic microorganisms. In Yellowstone National Park, the thermoacidophilic alga *Cyanidioschyzon* exhibits an annual seasonal biomass fluctuation referred to as 'mat decline', where algal viability decreases as ultraviolet and visible irradiances increase during summer. We examined the role irradiance might play in mat decline using irradiance filters that uncouple ultraviolet and visible effects along with custom microarrays to study gene expression *in situ*. Of the 6507 genes, 88% showed no response to ultraviolet or visible, implying that at the biomolecular level, these algae inhabit a chemostat-like environment and is consistent with the near constant aqueous chemistry measured. The remaining genes exhibited expression changes linked to ultraviolet exposure, to increased visible radiation, or to the apparent combined effects of ultraviolet and visible. Expression of DNA repeti-tive elements was synchronized, being repressed by visible but also influenced by ultraviolet. At highest irradiance levels, these algae reduced transcription of genes encoding functions involved with DNA replica-tion, photosynthesis and cell cycle progression but exhibited an uptick in activities related to repairing DNA damage. This corroborates known physiological responses to ultraviolet and visible radiation, and leads us to provisionally conclude that mat decline is linked to photoinhibition

Introduction

The Cyanidiales are an order of unicellular eukaryotic red algae that thrive in acidic (pH 0.2–4.0) and high tempera-ture (38–56°C) geothermal environments. No other phototrophic microorganisms are known to inhabit this combination of environmental conditions resulting in an ecological niche specific for these algae. Three genera are currently recognized and include *Cyanidium*, *Galdieria* and *Cyanidioschyzon* (Albertano *et al*., 2000), which as a group are a visually dominant component of microbial communities in high temperature acidic environ-ments. In addition to contributing to primary productivity in such extreme environments, the Cyanidiales also partici-pate in the biogeochemical cycling of arsenic and mercury (Kelly *et al*., 2007; Lehr *et al*., 2007a; Qin *et al*., 2009).

Lehr and colleagues (2007b) followed *Cyanidioschyzon* population dynamics over an annual cycle in Yellowstone National Park (YNP) and reported a phenomenon they termed 'mat decline'. Mat decline is marked by a signifi-cant loss in algal viability, which corresponds to the mat changing from a thick, dark green assemblage during the winter months to a light green, greatly thinned biofilm during the summer months (Lehr *et al*., 2007b). Mat decline was not linked to shifts in water chemistry, as near chemostat-like conditions prevailed with respect to aqueous constituents over time and across seasons (Lehr *et al*., 2007b). Rather, mat decline was found to correlate primarily with changes in ultraviolet (UV) irradiance and/or visible (VIS) light intensity.

While solar irradiance powers algal photosynthesis, it also represents an important source of stress. Few studies have sought to elucidate mechanisms underlying cyanidial response to this type of stress and those studies have been confined to pure cultures in laboratory settings (Minoda *et al*., 2005; 2010). Developing and applying molecular tools for *in situ* analyses are therefore critical next steps needed to elucidate the mechanisms by which the Cyanidiales respond to environmental change in nature. Several genomic resources are available for these

algae, including the complete genome sequence of *C. merolae* strain 10D and an expressed sequence tag (EST) data set for *G. sulphuraria* (Matsuzaki *et al*., 2004; Weber *et al*., 2004). These organisms and their genomes have been used as models for studying algal origin and evolution, as well as for investigating basic regulatory mechanisms in photosynthetic eukaryotes (Fujiwara *et al*., 2009).

With the genomic tools available, it is now possible to study Cyanidiales gene expression *in situ* at the level of the whole transcriptome, which could potentially lead to a more comprehensive understanding of Cyanidiales physiological ecology in general, and of the mechanisms underlying the mat decline event in particular. The present study employed a custom oligonucleotide microarray, designed from genome sequences of site-relevant YNP *Cyanidioschyzon*, to examine genetic responses of *Cyanidioschyzon* to UV and VIS irradiance *in situ*. Gene expression patterns were monitored over an annual cycle in relation to seasonal variation in both UV and VIS intensities. To uncouple the effects of UV and VIS radiation, gene expression was also examined in the presence and absence of UV filters The gene expression patterns uncovered provide an ecologically relevant molecular framework for understanding the mat decline event, as well as for providing greater insight into *Cyanidioschyzon* natural history.

Results

Environmental context

Lemonade Creek was selected for this study because of the robust microbial mats (Fig. S1A) formed by the *Cyanidioschyzon* algae. In previous 18S rRNA and *rbcL* phylogenetic surveys of this location and other Cyanidiales habitats in YNP, we have only encountered *Cyanidioschyzon* phylotypes in aqueous geothermal environments (Lehr *et al*., 2007b; Toplin *et al*., 2008; Skorupa *et al*., 2013). Ready access to these lush green mats enabled rapid sampling and processing of biomass used to recover mRNA for transcript analysis. Throughout the samplings, the algal mats were constantly submerged (3–5 cm) by creek flo and subjected to either one of two irradiance filte treatments (UF5- or OP4-type filters) which were arranged in pairs and in triplicate. The UF5 filte transmits about 90% of the visible spectrum, roughly 5% of the near-UVA spectral region and less than 0.1% in the UVB region. The OP4 filte transmits about 90% of the visible and near-infrared spectrum (400 ≥ 800 nm) and about 80–90% of the UVA/UVB region (i.e. 280–400 nm). The paired UF5 or OP4 filter were arranged away from the creek bank so as to avoid potential edge effects but were optimized with respect to maximal algal mat growth for biomass harvest (Fig. S1A).

To document seasonal environmental conditions as well as those encountered at the time of biomass collection for microarray analyses, measurements of UVA (315–400 nm, primary frequency sensitivity from 368 to 374 nm), UVB (280–315 nm, primary frequency sensitivity 294 nm, but with 50% response at 312 nm) and VIS (400–700 nm, primary frequency sensitivity at 555 nm) irradiance, water temperature, and aqueous chemistry were either continuously recorded with instrumentation installed in the fiel or measured with portable equipment. Sporadic VIS data loss occurred due to either equipment malfunction during extreme weather conditions or wildlife tampering (primarily grizzly bears, Fig. S2). However, even with the data gaps, seasonal trends in solar irradiance levels changed in an expected temporal fashion (Fig. 1A). Highest intensities were measured from late-June through August, with UVA readings peaking at 33.4 W m^2, UVB at 1.3 W m^2 and maximal VIS levels of 869.6 W m^2. Also as expected, lowest daytime irradiance values were recorded near the winter solstice, decreasing to 16.6 W m^2 for UVA, 0.2 W m^2 for UVB and 10.8 W m^2 for VIS. Accurate winter VIS readings were at times obscured due to periods of extensive snow cover that blocked the VIS sensor deployed at the fiel site (e.g. Julian days 6–21, Fig. 1A). For logistical reasons, fiel site visits during the winter months were less frequent, and therefore, removing snow cover from the VIS sensor was not optimum with respect to data acquisition. However, point measurements obtained with a portable radiometer on biomass sampling days demonstrated that during the winter months, VIS levels were more than an order of magnitude lower than in summer (Fig. 1A).

Water temperature changes were modest, increasing from 46 to 54°C during the seasonal sampling points (Fig. 1B, but see later discussion). Aqueous chemistry was measured from water samples taken directly above the algal mats. Most chemical constituents showed relatively low levels of variation when examined monthly over the approximate 2-year sampling period (Table 1). Concentrations and variations for the four specifi time points included in the microarray analysis were quite similar to the long-term trends. Na, Si, Ca, Mg, Fe and SO_4 were all very stable, displaying coefficients of variation of 0.1–6.3% (Table 1). Al, Mn, Cl^- and F^- were more variable during the 20-month monitoring period as well as on the four specifi sampling dates chosen for microarray analysis (coefficients of variation = 17.1–28.1%). In general, however, there were no obvious trends but rather random oscillations between sampling dates. With the analytical methods employed, concentrations of NO_3^- and PO_4^{2-} were below detection; however, previous work at this site determined that NO_3^- levels in the three thermal tributaries comprising Lemonade Creek averaged 8.9 μM, while PO_4^{2-} averaged 65 nM (Mathur *et al*., 2007).

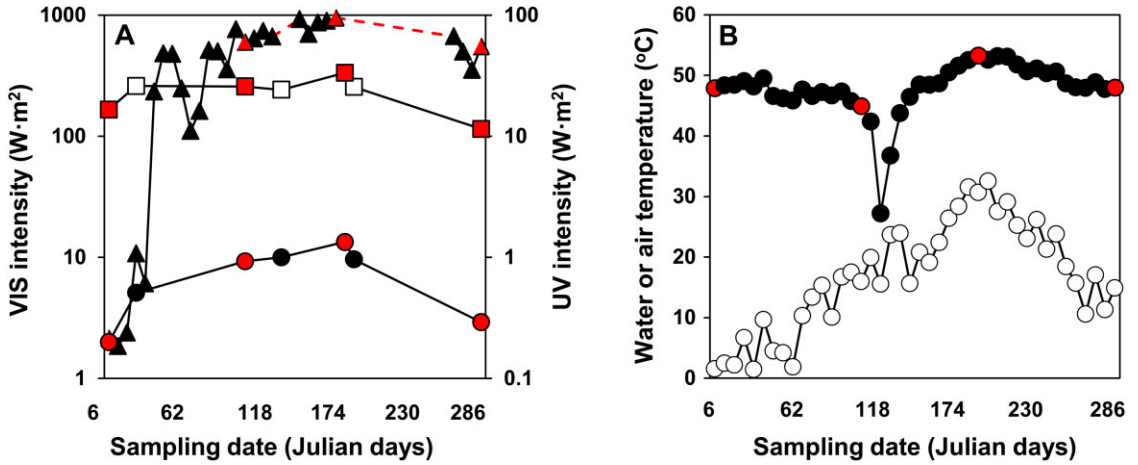

Fig. 1. Temporally intensive measurements of irradiance and temperature at Lemonade Creek.
A. UVA (315–400 nm, □), UVB (280–315 nm, ●) and VIS light (400–700 nm, ▲) intensity as a function of time (shown in Julian days). VIS light intensity data points are the average of seven maximum daily point readings recorded over the course of a week. To account for differences in seasonal photoperiod length, only visible light measurements recorded between the hours of 8 AM and 4 PM were used to calculate the daily maximum. Discontinuities in visible light recordings, as a result of either equipment malfunction or wildlife tampering, are displayed as dashed red lines between data points. UV irradiance was measured in the fiel with a portable radiometer.
B. Water temperature (●) and air temperature (○) measurements as a function of time (shown in Julian days). Temperature data are the average of seven maximum daily point readings recorded over the course of a week. The sharp decrease in water temperature reflect spring snowmelt at Lemonade Creek. Measurements recorded for UV-VIS intensity (A) and water temperature (B) on the days of *Cyanidioschyzon* microarray sample collection are illustrated as fille red symbols.

An important exception to the temporal consistency of the water temperature and chemistry occurred during spring snowmelt (e.g. late April to early May, depending on the start of spring run-off), when the physical (e.g. temperature, Fig. 1B) and chemical properties of the creek water changed dramatically. Low water temperatures were due to Lemonade Creek serving as the primary drainage route for the canyon in which it is located. Following sustained air temperatures above 16°C (~Julian day 104), significan decreases in water temperature (~27°C) were observed (Fig. 1B), corresponding to frigid snowmelt mixing with the geothermal water. Spring run-off

Table 1. Aqueous geochemistry of Lemonade Creek during a 20 month monitoring period and at the four time points when algal biomass was sampled for microarray analysis.

	Concentration (mM unless otherwise noted)					
Constituent	All monthly sampling ($n = 20$)	November 2009	January 2010	April 2010	July 2010	Microarray sampling months ($n = 4$)
pH	2.76 ± 0.11	2.78	3	2.43	N/A	2.74 ± 0.29
Element						
Na	2.10 ± 0.10	2.25	2.08	2.27	2.01	2.15 ± 0.12
Si	4.57 ± 0.26	4.69	4.48	4.73	4.23	4.53 ± 0.23
K	0.67 ± 0.04	0.69	0.66	0.70	0.63	0.67 ± 0.03
Ca	0.22 ± 0.04	0.21	0.20	0.19	0.20	0.201 ± 0.002
Mg	0.085 ± 0.006	0.083	0.078	0.081	0.078	0.080 ± 0.003
Al	0.434 ± 0.104	0.307	0.307	0.361	0.439	0.35 ± 0.06
Fe	0.055 ± 0.003	0.057	0.052	0.054	0.056	0.055 ± 0.002
As	B/D (0.67)[a]	B/D (0.67)	B/D (0.67)	B/D (0.67)	B/D (0.67)	B/D (0.67)
P	B/D (0.53)	B/D (0.53)	B/D (0.53)	B/D (0.53)	B/D (0.53)	B/D (0.53)
Mn	2.38 ± 0.27 μM	2.29 μM	2.20 μM	3.38 μM	2.20 μM	2.52 ± 0.57 μM
Zn	2.23 ± 0.47 μM	1.97 μM	2.28 μM	1.20 μM	2.34 μM	1.95 ± 0.52 μM
Ion						
Cl^-	0.63 ± 0.18	0.88	0.56	0.46	0.664	0.64 ± 0.18
NO_3^-	B/D (0.32)	B/D (0.32)	B/D (0.32)	B/D (0.32)	B/D (0.32)	B/D (0.32)
SO_4^{2-}	7.38 ± 0.68	7.16	8.18	7.2	7.53	7.52 ± 0.47
F^-	20.8 ± 6.0 μM	17.3 μM	17.2 μM	17.3 μM	27.6 μM	19.9 ± 5.2 μM

a. Values in parenthesis are the detection limits (in μM) for constituents that fell below the detection limit using either the inductively couple plasma optical emission spectrometry or anion exchange chromatography. All values are shown as the mean ± 1 standard deviation. B/D, below detection, N/A, not available.

also resulted in high water volume, which scoured the creek sediments and swept away the algal mats. Consequently, high snowmelt periods were excluded from microarray analysis. Subsequent to spring snowmelt, water temperatures increased rapidly (Fig. 1B) due to the creek flo being exclusively comprised of water from the geothermal tributaries. This reestablished optimum growth conditions and resulted in lush algal mats (e.g. Fig. S1A). Following recolonization, water temperatures continued to rise, peaking at 54°C after the summer solstice (Julian day 172), which coincided with maximal summer air temperatures (Fig. 1B).

Transcript levels for most algal genes do not vary across seasons

A striking feature of the microarray data set was that the transcript levels of 88% of the 6507 genes analysed did not increase or decrease by greater than twofold across seasons. At the organismal level, this indicates that the creek environment provides near chemostat-like growth conditions for *Cyanidioschyzon* spp. and is consistent with the very stable aqueous chemistry measurements (Table 1) and only modest changes in temperature. The major abiotic variable in this environment consists of seasonal changes in solar irradiance.

Irradiance-linked changes in gene expression

Gene expression was examined in four ways (Table 2). Our firs analysis assessed the relative effects of UV presence versus UV absence for each gene in a pairwise comparison, where gene transcript levels in OP4-filtere algal mats (exposed to VIS + UV and referred to as + UV) were compared with UF5-filtere mats (VIS-only exposed and referred to as –UV) at all four seasonal sampling time points. A second analysis focused on VIS-specifi gene transcript levels by comparing peak seasonal irradiance (July) versus lowest seasonal irradiance (January) for cells only exposed to VIS irradiance (Table 2). A third analysis inferred UV-specifi changes in gene transcript levels by identifying genes whose July : January transcript ratio differed significantl in VIS + UV mats but not in VIS-only mats. Our fourth analysis identifie genes that appeared to be influence by both VIS and UV. These genes were distinguished as having July : January transcript ratios that differed significantl in both types of irradiance-treated mats (VIS + UV and VIS-only) but whose ratios significantl differed between filte treatments. For all types of transcript abundance ratio analyses, transcript pool size reflect transcription and turnover. Statistically significan differences (primarily P-values ≤ 0.05) are reported as $\pm \log_2$, with $\geq$ twofold positive gene transcript ratios inferred to represent gene up-regulation, whereas $\geq$ twofold negative ratios were interpreted as representing down-regulation.

Analysis I: expression changes linked to the presence or absence of UV

Apparent gene expression responses attributable to UV were most evident in January 2010 (Fig. 2), where the transcript levels of 182 genes were statistically signifi cantly different in + UV algal mats. The majority (92%) of the UV-sensitive genes at this time point exhibited reduced expression (Fig. 2), with most annotated as DNA repetitive elements (DREs) (Table S1). Somewhat surprisingly, apparent UV-linked expression patterns were far less evident during July 2010 (Fig. 2), when UV levels are

Table 2. Summary of gene expression analyses.

Analysis	Time points	Filter treatments	Irradiance	Notes
I. Transcript abundance in relation to presence or absence of UV	Nov-Jan-Apr-July	OP4 and UF5	VIS + UV mats versus VIS-only mats	Comparing each gene in +UV versus –UV mats across all seasons (+UV : –UV transcript ratios)
II. VIS-specifi	July versus January (Max versus Min VIS)	UF5	VIS-only	July : January transcript ratios in mats only exposed to VIS (UF5 filtere mats)
III. UV-specifi	July versus January (Max versus Min UV)	OP4 and UF5	VIS + UV mats compared against VIS-only mats	July : January transcript ratios in mats exposed to VIS + UV (OP4 filtere mats), but not significantl expressed in VIS-only mats (UF5 filtere mats)
IV. UV interactions with VIS	July versus January (Max versus Min VIS and UV)	OP4 and UF5	VIS + UV mats compared with VIS-only mats	July : January transcript ratios in both VIS + UV (OP4 filtere mats) and VIS-only mats (UF5 filtere mats), identifying genes whose transcript ratios in VIS + UV mats are significantl different (+/–) than VIS-only mats

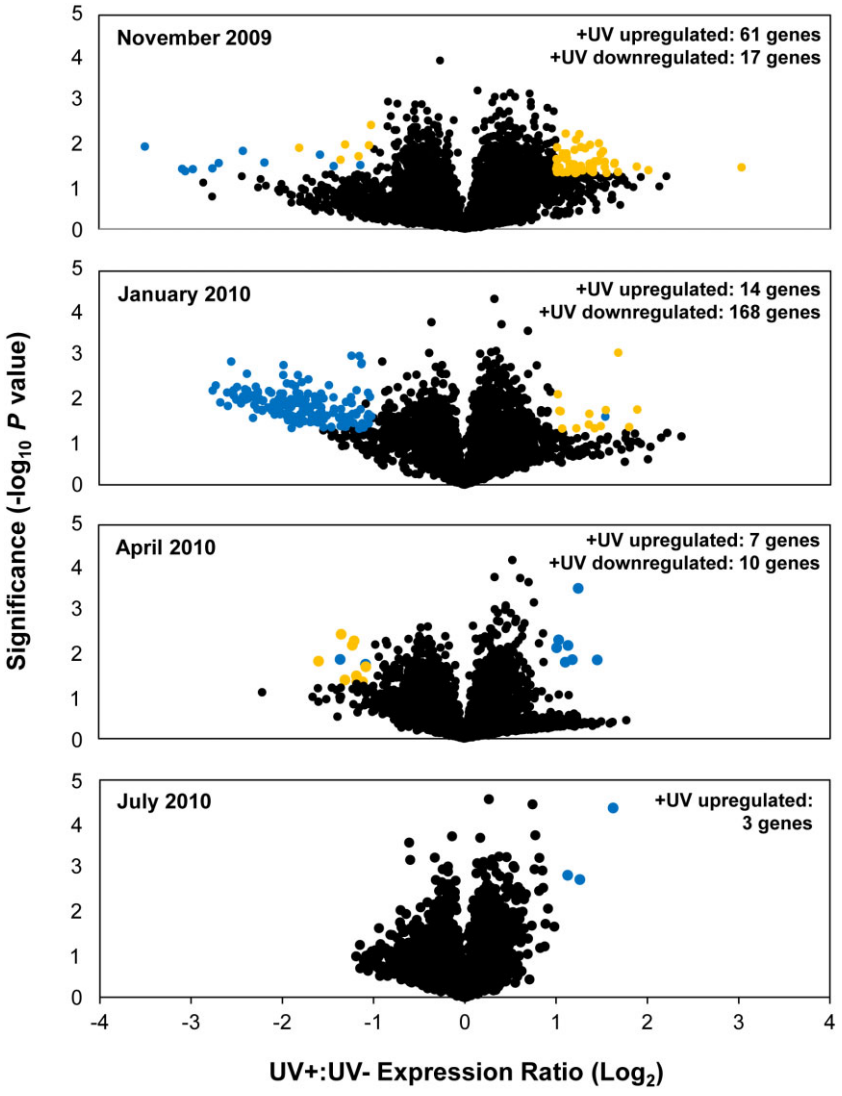

Fig. 2. Volcano plots of *Cyanidioschyzon* gene expression response to UV exposure at four time points, showing $\log_2$ ratios of UV+ : UV– expression. Relative expression values are plotted against the –log of *P*-values from *t*-tests used to identify statistically significan differences in transcript abundance. In all plots, genes with a non-significan UV+ : UV– expression ratio are shown as black dots, nuclear-encoded genes with statistically significan expression ratios (≥ twofold-change; *P*-value ≤ 0.05) are illustrated as blue dots, and plastid or mitochondrial-derived genes with significan UV response (≥ twofold-change; *P*-value ≤ 0.05) are depicted as yellow dots.

highest (Fig. 1A) and mat decline effects are visually evident (Fig. S1B; Lehr *et al*., 2007b). At this time point, only three genes exhibited significantl different transcript pool sizes in response to UV change, with all being up-regulated between twofold and threefold (Fig. 2; Table S1). One of these genes (CMR353C) is annotated as coding for a homologue of a protein involved in respiratory burst response, a well-known plant defence mechanism activated during pathogen infection events (Sagi *et al*., 2004). The two others are annotated as coding for hypothetical proteins (Table S1).

During transitional UV intensity periods (November 2009, UV levels decreasing; April 2010, UV levels increasing), the total number of genes whose transcript levels showed UV-related changes decreased markedly, even when seasonal irradiance intensifie (Fig. 1A). In the Spring (April 2010), 17 genes significantl changed in expression in the presence of UV, with the majority (59%) down-regulated (Fig. 2, Table S1). These included components of the translational machinery (ribosomal proteins *rps4*, *rps12*, *rpl5*, *rpl32*) (Table S1) and a chloroplast-encoded translation initiation factor *infB* (Table S1). In the Fall (November 2009), components of the translational machinery also showed statistically significan +UV : –UV transcript ratios, although the translation-related genes were not uniformly repressed. Specificall , nuclear-encoded ribosomal subunit proteins (*rpl23A*, *rpl34*, *rpl35A*), a ribosome biogenesis enzyme (*rio1*), and a eukaryotic translation initiation factor (*eIF-1*) exhibited twofold to eightfold greater transcript levels in +UV mats, while expression of a chloroplast-derived small ribosomal protein (*rps18*) displayed a roughly sixfold decrease in +UV algal cells (Fig. 2; Table S1). Fall UV-linked expression analyses further revealed that all up-regulated genes ($n = 61$) were nuclear-encoded (Fig. 2), while of all down-regulated genes ($n = 17$), 65%

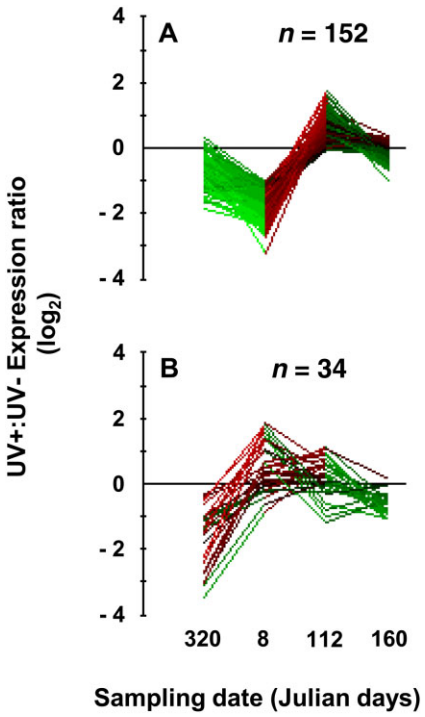

Fig. 3. *K*-means clustering analysis of UV+ : UV– expression ratio profile for two gene clusters in response to seasonal UV irradiance shifts. The data are plotted as the $\log_2$ fold-change across the four time points illustrated as red-fille symbols in Fig. 1. Red and green colours depict positive and negative UV+ : UV– expression ratios derived from analysis of algal mats exposed to UV (UV+) versus mats shielded from UV (UV–).

were either plastid or mitochondrial (Fig. 2; Table S1). UV exposure in Fall also coincided with a systematic reduction in expression of the electron transport apparatus, including transcripts for cytochrome b6-f (*petG*, *petM*), nicotinamide adenine dinucleotide, reduced (NADH) dehydrogenase (*nad1*), cytochrome c oxidase (*cox1*, *cox2*) and cytochrome c reductase (*cytB*) (Table S1).

A *k*-means clustering analysis grouped genes according to similarities in their apparent expression profile across seasons (Fig. 3). Analysis began with November 2009 and progressed to July 2010 during which time UVA irradiance levels increased from 13.1 to 33.4 W m^2, UVB from 0.28 to 1.34 W m^2 and VIS from 80 to 869 W m^2 (Fig. 1A). For a gene to be included in a cluster, its expression needed to be similar to the group across the four seasonal time points and a statistically significan change in the +UV : –UV transcript ratio was required for at least one of the time points. With these selection criteria, k-means clustering revealed several gene clusters responding to UV, although only two are discussed here. Gene cluster A (152 genes) was dominated (84%) by genes coding for DREs (Fig. 3A; Table S2), class I elements (retrotransposons) (CMF037X, CMK165C, CMP121C) and a class II element (transposon) (CMO148C). As a group, their +UV : –UV transcript ratios suggested reduced expression in response to declining UV in Fall (Nov 2009) and Winter (Jan 2010) (Fig. 3A). As solar irradiance increased in the Spring (April 2010) (Fig. 1A), +UV : –UV transcript ratios increased (Fig. 3A). However, at peak Summer UV irradiance (July 2010) (Fig. 1A), the apparent transcription response tended towards neutral with regards to UV exposure (Fig. 3A), consistent with the transcriptome as a whole (Fig. 2).

Cluster B consisted of 34 genes (Fig. 3B; Table S2) and included 10 genes coding for functions involved in aspects of oxidative phosphorylation, seven for ribosome structure and two for photosynthesis (Table S2). As a group, expression of cluster B genes tended to be enhanced by UV in Winter and Spring; interestingly, UV effects were muted during the highest UV season (July 2010), as observed for cluster A (Table S2). Although mean apparent transcriptional responses within the respective clusters appeared synchronous, transcript abundance differences for genes within each cluster sometimes were not statistically significan because of variability among biological replicates. This was particularly evident for the UV transition periods of Fall and Spring for Cluster A (data not shown).

Analysis II: expression changes specificall linked to seasonal changes in VIS irradiance

Analyses of gene expression based on presence or absence of UV suggested that potentially (an)other environmental factor(s) might also be influencin gene expression, perhaps even dampening UV influence (Fig. 2; Fig. 3). Because VIS irradiance differed by more than an order of magnitude between Summer and Winter (Fig. 1A), we compared gene transcript levels in mats only exposed to VIS during the period of highest intensity (July 2010) versus that of lowest intensity (January 2010).

In comparing transcripts between January and July, of the 275 VIS-only responsive genes (Table S3), transcript abundance was depleted in 158 and increased in 117. Down-regulated genes encoded functions associated with DNA replication and repair (Fig. 4), porphyrin and chlorophyll metabolism, cell cycle activities, and a large contingent of DREs and retrotransposable elements (Fig. 4; Table S3). Cellular functions inferred to be enhanced by increased VIS included electron transport (four genes), adenosine triphosphate (ATP) synthesis (two genes) and two genes annotated as coding for functions associated with photosynthesis [Photosystem II 10 kDa phosphoprotein (*psbH*) and Ferredoxin (*petF*)] (Fig. 4; Table S3).

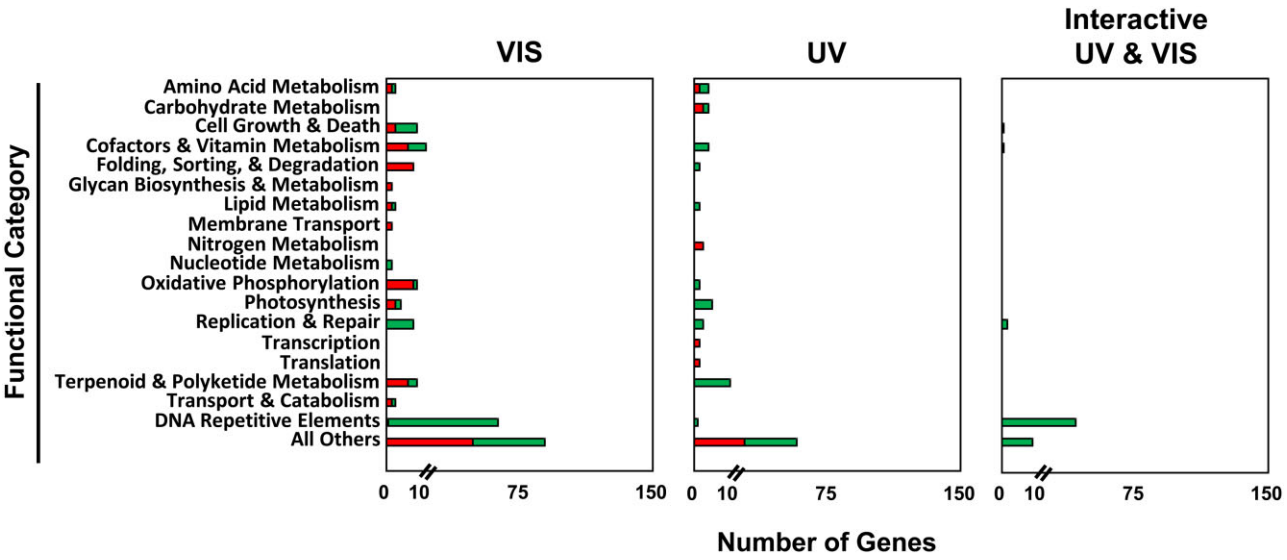

Fig. 4. Functional characterization of gene expression sensitivity occurring as a result of VIS, UV or what appear to be interactive effects of UV and VIS. Shown are the functional role categories for genes significantl up- (red bars) or down-regulated (green bars) in response to increasing seasonal irradiance. Gene expression responses were determined by comparing high irradiance (July 2010) to low irradiance (January 2010) time points under either the UV+ or UV– algal mats.

Analysis III: expression changes specificall linked to seasonal changes in UV irradiance

Significan July : January transcript ratios in VIS + UV mats were compared with those in the VIS-only mats to identify genes exhibiting significan expression differences when exposed to both VIS and UV but not when only exposed to VIS. These expression changes (plus or minus) were therefore interpreted as associated with a greater than fivefol increase in UV irradiance. Up-regulated functions included carotenoid biosynthesis (ZDS), a DNA photolyase (CmPHR5) and a radical scavenging enzyme involved in stress response [glutathione-S-transferase (GST)] (Fig. 4; Table S4). Apparent down-regulated genes in this group involved growth and energy production, including translation initiation and elongation (three transcripts), ribosome formation (fiv transcripts), DNA replication (two transcripts), light-harvesting (two transcripts) and the light-dependent pathways of photosynthesis (two transcripts) (Fig. 4; Table S4).

Analysis IV: expression changes apparently affected by UV-VIS interaction

Many genes exhibited significan July : January transcript ratios in the VIS-only as well as in the VIS + UV mats. In a number of instances, however, the VIS-only transcript ratio was significantl altered (+ or –) in VIS + UV mats, suggesting that for these genes, inclusion of UV signifi cantly shifted transcript levels relative to VIS alone and indicating some type of UV-VIS interaction. This included 68 genes (76% DREs) that exhibited a negative July : January ratio in the VIS-only algal mats, but when in the presence of UV irradiance (VIS + UV mats), the apparent VIS repression was weakened or abolished (Fig. 4; Table S5). For another group of 10 genes, UV exposure appeared to accentuate VIS repression, making the VIS + UV July : January transcript ratios more negative relative to VIS-only (Table S5). In this latter group, one cell function relevant to mat decline involved DNA replication (Table S5).

DRE characterization

Given the significan influenc of UV and VIS on DRE transcript levels (Fig. 3A; Fig. 4; Tables S1–S3 and S5) and the documented involvement of DREs in plant cellular response to environmental cues such as pathogen attack or physical damage (Grandbastien *et al.*, 1997; Schmidt and Anderson, 2006), we next sought to classify the expressed DREs based on TBLASTX sequence similarity searches against Repbase (Jurka *et al.*, 2005), a database of eukaryotic repetitive elements. While a large portion (42%) could not be assigned to a repeat family, the remainder contained one or more known repetitive element fragments. *Gypsy*-type long-terminal repeat (LTR) retrotransposons were the dominant family identifie (Table 3), of which nearly 71% were found to respond to VIS irradiance effects in the July : January comparison. Members of the *MuDR* DNA transposon family were also detected (Table 3); these elements are known to function as the regulatory element for the *Mu* family of DNA transposable elements (Lisch, 2002), the most active and abundant transposon found among all plant species (Liu

Table 3. Summary of repetitive element classificatio based on TBLASTX sequence similarity searches against Repbase.

Class	Family	VIS	UV	Interactive UV & VIS
LTR retrotransposon				
	Unknown			2
	BEL	3		3
	Copia	6		7
	DIRS	2		1
	Gypsy	41		17
		52		30
Non-LTR retrotransposon				
	Unknown			1
	Daphne			1
	I			1
	Jockey	1		2
	L1	2		4
	Penelope	2		
	R1			2
	R2	1		
	RTEX	1		
		7		11
Endogenous retrovirus				
	Unknown		1	1
	ERV1			1
	ERV2	4		1
		4	1	3
DNA transposon				
	Unknown	1		
	EnSpm	2		
	Harbinger	2		
	hAT	5		3
	Helitron	2		1
	Kolobok	1		
	Mariner	1		
	MuDR	14	2	6
	piggyBac	1		
	Polinton	1	1	3
	Transib			1
		30	3	14

Columns represent repetitive elements significantl influence by either VIS, UV or what appear to be interactive UV and VIS effects.

et al., 2009). As with the LTR retrotransposons, the majority (66%) of *MuDR* transposons were responding to seasonal VIS irradiance effects (Table 3).

Discussion

The microarray-based analysis described here sought to understand the cellular events that underlie the *Cyanidioschyzon* mat decline event that we previously showed to be associated with high irradiance (Lehr *et al*., 2007b). The principal goal was to discover at the level of gene transcription how *Cyanidioschyzon* responds to changes in UV and VIS in nature and thus broaden our general understanding of Cyanidiales ecology. Prior to the current study, whole-community microbial gene expression has primarily employed metatranscriptomic profilin via cDNA pyrosequencing. Poretsky and colleagues (2005) pioneered this approach in a study of fresh water and marine bacterioplankton samples. This was followed by other studies of planktonic marine microbes (e.g. Shi *et al*., 2009; Ottesen *et al*., 2011; Stewart *et al*., 2011) and of *Leptospirillum* spp. biofilm and planktonic cells in the Rio Tinto system (Moreno-Paz *et al*., 2010). Microarrays have been employed to study sulphur-related differential gene expression by *Roseobacter* (Rinta-Kanto *et al*., 2010), to investigate bacterial and archaeal gene expression in relation to salinity gradients in the Columbia River coastal margin (Smith *et al*., 2010), and to discover growth-habit-related expression differences in biofil versus planktonic *Leptospirillum* spp. (Parro *et al*., 2007).

Because the custom microarrays utilized in the present work were designed from genomes of *Cyanidioschyzon* sp. isolated from the YNP geothermal features Lemonade Creek (CCMEE 5578) and Dragon Spring (CCMEE 5508), we view them as containing ecologically relevant gene sequences. Moreover, our study system presented an optimal setting for transcript profil studies for the following reasons: (i) algal biomass was abundant and could be acquired in seconds, providing confidenc that the transcript profile accurately reflecte mRNA pools at the time of sampling and obviating the need for secondary RNA amplification (ii) biomass sampling dates were separated by months, which allowed for complete mat re-establishment (occurs typically within 7–10 days) under the installed irradiance filte treatments; (iii) mat community function was not disrupted by the filter used to manipulate specifi irradiance wavelengths; and (iv) cDNA synthesis from polyA-tailed mRNA strongly biased the analysis to eukaryotic mRNA. Further, the Lemonade Creek chemical environment was chemostat-like during the biomass sampling period (and remains so), as judged from the temporally extensive examination of creek aqueous chemistry (Table 1). In the event of aqueous chemical fluctuations however, the fiel design allowed for all sampled mats to experience the same changes and thus was normalized across biological replicates. Of relevance to our previous work on arsenic methylation in *Cyanidioschyzon* strain 5508 (Lehr *et al*., 2007a; Qin *et al*., 2009), we note that the *arsM* genes that encode arsenic methyltransferase were routinely observed to be expressed and devoid of irradiance treatment effect.

Increased water temperatures in July 2010 (Fig. 1B) represented a potential stress for these algae (Brock and Darland, 1970) and as such could have influence gene expression across seasons (i.e. July vs. January). However, at each sampling, water temperature varied by no more than 0.5°C across the entire paired filte treatment sampling area (data not shown), and so temperature was likewise normalized at each sampling time point for the +UV : −UV expression comparisons. In summary, the

array design, the study site and the targeted microbial community represented an ideal combination of experimental conditions for studying gene expression *in situ* and in response to a specifi environmental factor, in this case solar irradiance.

Irradiance levels changed in an expected temporal fashion (Fig. 1A). Based on the +UV : −UV transcript ratios, *Cyanidioschyzon* was most sensitive to UV in November 2009 and January 2010 (Fig. 2), periods of the year when absolute UV levels were lowest (Fig. 1A) and algal mat structure most robust. As the study progressed into summer and both UV and VIS irradiances increased, the frequency of statistically significan +UV : −UV expression ratios declined, suggesting that other environmental influence were masking, overwhelming or muting UV effects. This was evident from whole transcriptome analysis (Fig. 2) as well as from the *k*-means clustering analysis (Fig. 3). Alternatively or in addition, the apparent lack of UV effects may reflec an overall enhanced cellular capacity to attenuate the harmful effects of UV.

Subsequent analyses comparing transcript levels during the highest (July 2010) and lowest (January 2010) irradiance periods revealed gene expression responses to VIS, UV and what appeared to be interactive effects of UV and VIS. The ~80-fold increase in VIS irradiance in July 2010 (relative to January 2010) corresponded to reduced expression of several examples of genes that encode functions related to porphyrin and chlorophyll metabolism, DNA replication, and cell and organelle division (Fig. 4; Table S3). A reduced capacity for cells to replicate DNA and divide, and to synthesize porphyrin and chlorophyll is consistent with the summer mat decline phenomenon (Fig. S1B; Lehr *et al*., 2007b) and suggests that photoinhibition may be a major causal factor (Long *et al*., 1994; Takahashi and Murata, 2008). Repression of the chloroplast *ftsZ* (Table S3) gene during periods of peak VIS irradiance is particularly interesting in relation to previous studies with light-synchronized *C. merolae* cultures where plastid and mitochondrial *ftsZ* genes were identifie as marker genes for S (synthesis)-phase cells, and with maximal expression and FtsZ accumulation correlating to dark cycle cells (Nishida *et al*., 2005; Fujiwara *et al*., 2009). The earlier observations are consistent with reduced photosynthetic productivity observed in high irradiance laboratory studies of *G. sulphuraria* (Oesterhelt *et al*., 2007). They are also consistent with other algae pure culture transcriptome studies illustrating the photorepression of the light-harvesting antenna of photosystem II in the psychrophilic diatom, in *Chaetoceros neogracile* (Park *et al*., 2010) and in *Haematococcus lacustris* (Kim *et al*., 2011).

Gene up-regulation in response to increased VIS was also apparent and seemingly involved the induction of several genes associated with oxidative phosphorylation, including cytochromes B and C, NADH ubiquinone oxidoreductase and terpenoid-quinone biosynthesis (Fig. 4; Table S3). This observation suggests increased respiration *in situ* and is consistent with studies of pure culture phototrophs exposed to irradiance stress (Huang *et al*., 2002; Park *et al*., 2010; Kim *et al*., 2011). Up-regulation of heat shock/chaperone genes in response to VIS-induced damage agrees with earlier studies demonstrating induction of the heat shock response following high-intensity VIS exposure and damage to PSII (Schroda *et al*., 2001; Yokthongwattana *et al*., 2001; Huang *et al*., 2002). High VIS dosage during the summer period likely involves the activation of repair mechanisms that function to protect PSII from VIS-induced photoinhibition.

In addition to VIS effects, gene regulatory pathways inferred to be UV-responsive involved the coordinated repression of genes involved in photosynthesis (Table S4). UV-linked reduced photosynthetic activity is also consistent with visual evidence of mat decline and our prior measurements showing evidence of reduced productivity in field-sample *Cyanidioschyzon* cells exposed to UV (Lehr *et al*., 2007b). The *in situ* data reported herein stand in contrast with laboratory studies with the cyanobacterium *Synechocystis* sp., where increased photosynthetic activity was observed in short-term (0.33–2 h) UV inductions (Huang *et al*., 2002). Other studies examining cyanobacterial UV responses have reported activation of a variety of protective and/or counteractive mechanisms, including negative phototaxis, DNA repair and production of photoprotective chemicals (Pattanaik *et al*., 2007). Increased expression of a cryptochrome DASH homologue (CmPHR5) in response to UV (Table S4) is consistent with that gene playing some role relevant to UV damage repair. Recently, the cloned *C. merolae* CmPHR5 protein was shown to provide cylobutane pyrimidine dimer repair and 100-fold increased UV resistance relative to controls (Asimgil and Kavakli, 2012). CmPHR5 exhibits maximum absorbance at 380, 420 and 450 nm (Asimgil and Kavakli, 2012) and thus is well suited for absorbing blue light. These properties illustrate that CmPHR5 is similar to cryptochromes, which are photoreceptors with a two-peak action spectrum, one in the blue-light region and the other in the UVA region (Senger, 1984), and which share significan homology with photolyases (Sancar, 2003; Lin and Todo, 2005). In plants, cryptochromes appear to act solely as transcriptional regulators of growth and development (Lin, 2000); by contrast, in the marine diatom *Phaeodactylum tricornutum*, cryptochromes demonstrate both DNA repair and transcription regulatory activities (Coesel *et al*., 2009). We note that several genes annotated as photolyases (CMD121C, CMH170C,

CMH274C, CMJ288C and CMO348C) were also up-regulated in response to seasonal UV, although they did not meet the twofold criterion imposed in this study. Active avoidance of UV and/or VIS is likely not a possible response for *Cyanidioschyzon* sp. as pure cultures of these particular YNP *Cyanidioschyzon* (Type IA; see Toplin *et al*., 2008) are not flagellated and their genomes do not contain identifiabl flagella assembly genes. Thus, active vertical migration within the mat structure would be constrained. Consequently, the gene expression patterns observed in this study should be viewed as an average of mRNA pools that span the vertical dimension of the entire algal mat, including cells experiencing reduced irradiance in the lower cell layers. This averaging effect would presumably be of less importance for the thinner, less robust mats of July 2010.

Expression of DREs was synchronous (Fig. 3A; Table S2) and repressed in reaction to VIS irradiance (Table S5), representing novel observations regarding possible DRE functions in algae. And while previous studies have suggested LTR, retrotransposons were absent from the nuclear genome of *C. merolae* strain 10D (Zhang *et al*., 2006; Nozaki *et al*., 2007), sequence similarity searches in this study annotated a significan number of the Yellowstone *Cyanidioschyzon* repetitive elements as containing *Gypsy*-type LTR retrotransposon sequences (Table 3). The importance of LTR retrotransposons has become increasingly appreciated (Zhang *et al*., 2006; Peddigari *et al*., 2008), as these elements can represent a large proportion of total plant genomes (Sormacheva and Blinov, 2011). In the context of function, we draw attention to a previous study linking altered LTR-retroelement transcription in response to UV irradiance stress response in plants (Ramallo *et al*., 2008). Our results suggest that increases in VIS irradiance decreased the *Cyanidioschyzon* DRE transcript pool, although the effects were season-specifi and complicated by UV intensity. July versus January transcript levels identifie UV repression of DREs during the low UV season (Fig. 2; Fig. 3A; Table S2), VIS-based repression during the high VIS irradiance periods (Fig. 4; Table S3) and apparent UV attenuation of the VIS repression (Fig. 4; Table S5).

In summary, the Cyanidiales are visually conspicuous as green mats or bands in acidic geothermal areas being found in soils (Pinto *et al*., 2007), endolithic rock layers (Gross *et al*., 1998; Yoon *et al*., 2006) and, in particular, aqueous environments (Brock, 1978; Gross *et al*., 2001; Toplin *et al*., 2008) such as that described in this study (Fig. S1A). Although phylogenetic surveys have documented their occurrence and their diversity in a variety of locales (Gross *et al*., 2001; Ciniglia *et al*., 2004) including Yellowstone (Ferris *et al*., 2005; Toplin *et al*., 2008; Skorupa *et al*., 2013), our understanding of Cyanidiales ecology remains rudimentary. The microarray data presented in this study begins to provide ecological context to what have largely been phylogenetic surveys (Ciniglia *et al*., 2004; Ferris *et al*., 2005; Yoon *et al*., 2006; Skorupa *et al*., 2013) and pure culture characterizations (Gross and Oesterhelt, 1999; Gross *et al*., 2001; Toplin *et al*., 2008). The high VIS and UV irradiance of Summer clearly represents a key ecological event for these algae, culminating in annual massive cell die-offs (Lehr *et al*., 2007b). Most genes (88%) were more or less equivalently expressed across all time points and showed no response to wide seasonal variation in solar irradiance. This serves to confir at a molecular level the aqueous chemistry evidence (Table 1) that these algal mats inhabit a chemostat-like environment. However, within this background, the microarray data also document how on a seasonal basis these algae shut down or reduce cell activities critical to DNA replication, photosynthesis, and the cell cycle, as well as exhibit apparent attempts to control or repair DNA damage. Our analysis did not examine translation level regulation, which presumably was at play in the algal cells, and it is not possible to entirely rule out possible regulatory responses to the 8°C temperature difference between seasons. However, based on the genes influence and seasonal expression patterns observed, we conclude that the mat decline event likely results from high VIS photoinhibition. Cellular responses to UV effects were also evident, sometimes appearing to interact with VIS through mechanisms that remain to be elucidated. This is particularly true for DREs, which responded in a coordinated manner to changes in VIS and UV, and which offer an inviting target for future investigations.

Experimental procedures

Site description, aqueous chemical analysis and biomass collection

All fiel experiments were conducted in YNP at the acidic geothermal feature Lemonade Creek (44°48′3.3″ N, 110°43′43.5″ W, spring number APTNN033 in the YNP thermal inventory) (Fig. 1) located in the Amphitheater Springs area. This site has been described previously (Mathur *et al*., 2007). Samples were taken on November 16, 2009; January 8, 2010; April 22, 2010; and July 9, 2010. Depending on travel conditions (e.g. winter snowmobile travel and snowshoeing vs. autotransport and normal hiking), biomass collection commenced at approximately 11:00 AM. Biomass was collected by transferring algal covered pebbles into sterile Falcon™ tubes along with creek water, vigorously shaking the tube by hand to dislodge the algal cells, transferring the algae to a sterile 15 ml Falcon tube and flash freezing the material in a dry-ice/ethanol bath. The entire process for each sample was completed within ~30–45 s. The frozen samples were then transported back to the lab on dry ice and stored at −80°C until used for RNA extraction.

A data-logger (Datalogger Spectrum 1000, Veriteq Instruments, Richmond, BC, Canada) equipped with a thermistor sensor cable was used to record hourly water and ambient air temperatures. Single point measurements were also recorded at the time of biomass sampling using a hand held thermometer or an Accumet AP110 portable temperature/pH meter (Fisher Scientific Pittsburgh, PA, USA), which was also used for pH determination. UV irradiance was measured at sampling times using an ILT-1700 radiometer (International Light, Newburyport, MA, USA) as previously described (Lehr *et al*., 2007b). Long-term hourly measurements of VIS radiation were recorded using a LI-1400 data-logger equipped with a pyranometer (LI-COR, Lincoln, NE, USA) that was installed at the fiel site.

Aqueous geochemistry was monitored throughout the entire sampling period. Briefl , site water was filter-sterilize (0.22 μm) directly into sterile 50 ml Falcon tubes. Some fil tered samples were acidifie (1.0 ml of 16 M HNO_3) in the fiel prior to transport and analysed for total dissolved elements. Major anions and cations were measured using anion exchange chromatography and inductively couple plasma optical emission spectrometry as described previously (Lehr *et al*., 2007b).

For the fiel experiments, two types of irradiance filterin materials were used in pairs and in triplicate (Fig. S1A). Both filte materials are transparent to photosynthetically active radiation. The OP-4 filte material (Cyro Industries, Woodcliff Lake, NJ, USA) transmits about 90% of VIS, and 80–90% of UVA and UVB radiation, whereas the UF-5 filte material (Autohaas N. Am, Philadelphia, PA, USA) transmits about 90% VIS but blocks 95% of all UVA and 99.9% of UVB spectra (Norris *et al*., 2002).

Microarray design

DNA sequences from 6528 genes were used as an input for microarray probe design. A total of 6282 nuclear, 213 plastid and 33 mitochondrial-encoded genes comprised the input sequences and were derived from two different sources. The primary source was genomic DNA from two ecologically relevant isolates originating from Dragon Spring (CCMEE isolate 5508) and Lemonade Creek (CCMEE isolate 5578), which were sequenced on a Solexa Genome Analyzer (Illumina, San Diego, CA, USA). Sequences were assembled to the *C. merolae* strain 10D reference genome using the Burrows-Wheeler Transformation alignment tool (Li and Durbin, 2009). Base calls made to generate consensus sequences were determined by ≥ 90% agreement from a minimum of 20 aligned sequences. Genome coding regions from both isolates were identifie with a BLASTn search against the *C. merolae* strain 10D genome database. Assembled sequences are available in the following GenBank SRA accessions: SRP030132 (isolate 5578) and SRP030133 (isolate 5508). Because the primary research site for the microarray study was Lemonade Creek, coding regions identifie in isolate 5578 were considered most important for inclusion in the probe design. Therefore, all full-length coding regions (6082 sequences) identifie in isolate 5578 were used in the custom microarray construction. Coding regions unique to isolate 5508 (isolated from Dragon Spring), as well as isolate 5508 DNA sequence that complemented gapped or non-full-length 5578 isolate sequences (313 sequences), were also included. A secondary source of sequence for the array design were open reading frame (ORF) sequences (133 sequences) either unique to the *C. merolae* strain 10D genome or sequences from the 10D genome that fille gaps in the 5508 and 5578 isolate genomes.

From the 6528 input sequences, 21 sequences were considered 'exemplars', meaning that quality probes could not be adequately designed. The fina array design included 6507 unique gene sequences incorporated into a 12-plex Nimblegen Systems (Madison, WI, USA) custom array. Five unique 60-mer oligonucleotide probes were designed per gene using a multistep approach to select for probes with optimal hybridization. All sequence probes with optimal hybridization properties were represented three times on each chip (i.e. three technical replicates per chip) for a total of 45 probes per gene. A large number of control probes, which had similar thermal properties as the input gene sequences, were also incorporated into the array design and used to quantify array background signal and non-specifi hybridization.

RNA preparation

RNA was extracted using a modifie version of the FastRNA Pro Soil-Direct Kit (MP Biomedicals, Solon, OH, USA). Frozen samples (~10 ml) were firs thawed on ice to the point of convenient removal from the Falcon tubes, transferred to prechilled 30 ml sterile Oakridge tubes, centrifuged (8000 × *g*, 5 min, 4°C) and washed twice with 10 ml of ice-cold 0.85% NaCl (wt/vol). The algal pellet was quickly weighed to normalize quantity of starting biomass (100 mg) and then rapidly suspended in 1 ml of RNA Pro Soil Lysis Buffer. Beginning with the FastRNA Pro Soil-Direct Kit, the suspension was transferred to a Lysing Matrix E tube and the RNA extraction continued according to the manufacturer's instructions.

Following extraction, RNA was DNase treated using a modifie version of the TURBO DNA-free kit (Ambion, Austin, TX, USA). Briefl , RNA was treated with 2 μl TURBO DNase per 50 μl sample volume and incubated at 37°C for 1 h. This process was repeated using 1 μl TURBO DNase per 50 μl sample volume and again incubated at 37°C for 1 h. RNA was purifie by one round of extraction with phenol-chloroform-isoamyl alcohol (25:24:1), and then precipitated by the addition of 2.5 volumes of 100% ice-cold ethanol (EtOH) and 0.1 volume of 7.5 M ammonium acetate (overnight at –20°C), followed by centrifugation. The RNA pellet was washed once with 70% ethanol and suspended in nuclease-free water. DNA was confirme to be absent by polymerase chain reaction (PCR) tests containing 100 ng of RNA preparation, GoTaq Flexi DNA polymerase (Promega, Madison, WI, USA), and the *rbc*L primers rbcL090F and rCR described previously (Yoon *et al*., 2002; Ciniglia *et al*., 2004).

Microarray sample preparation, labelling, hybridization and processing

The RNA from three replicate samples collected for each irradiance treatment was converted to double-stranded cDNA

using a modifie version of the SuperScript Double-Stranded cDNA Synthesis Kit (Invitrogen, San Diego, CA, USA). Briefl , 10 μl of total RNA and 1 μM oligo dT (22) primer (Integrated DNA Technologies, Coralville, IA, USA) were mixed, incubated at 70°C for 10 min and then transferred to an ice water slurry for 5 min. Dithiothreitol (10 mM), deoxynucleotide triphosphates (dNTPs) (0.5 mM) and one volume of first strand reaction buffer were added and incubated at 42°C for 2 min. Subsequently, 400 U of SuperScript II reverse transcriptase was added, and the mixture was incubated at 42°C for 1 h. The balance of the cDNA synthesis continued according to the manufacturer's instructions.

After synthesis, the double-stranded cDNA was purifie by one round of extraction with phenol-chloroform-isoamyl alcohol (25:24:1), followed by precipitation in 3 M NaOAc (pH 5.2), 2.5 volumes 100% ice-cold EtOH and 24 μg of glycogen, and incubated at −80°C overnight. After collecting the cDNA by centrifugation, the cDNA pellet was washed with 70% ice-cold ethanol, air-dried at room temperature for 10 min and suspended in nuclease-free water. The cDNA was cleaned using the Qiaquick PCR Purificatio Kit (Qiagen, Valencia, CA, USA) and assessed for purity using the RNA 6000 NanoChip assay on an Agilent 2100 Bioanalyzer (Agilent Technologies, Palo Alto, CA, USA).

Labelling was performed by mixing 1 μg of cDNA with 1 U μl^{-1} Klenow fragment and 1 U μl^{-1} Cy3 fluorophor and incubating at 37°C for 2 h. For each array, 4 μg Cy3-labelled cDNA was hybridized using the NimbleGen Hybridization Kit (NimbleGen Systems, Madison, WI, USA) according to the manufacturer's instructions. Arrays were scanned using a GenePix 4000B scanner (Molecular Devices, Sunnyvale, CA, USA) at a photomultiplier tube detector voltage of 550. Scanned images were aligned, background-corrected and normalized using a robust multichip average and NimbleScan software (NimbleGen Systems). The probe detection limit was define per array as being greater than four median absolute deviations (MADs) from the signal intensity of negative control probes included in the array design. Low intensity probes that fell below this baseline expression threshold were excluded from analysis.

Microarray data analysis

Gene transcript levels were extracted from the arrays using the FlexArray (version 1.6.1) software package available from Génome Québec (http://genomequebec.mcgill.ca/FlexArray). Probe signals were filtere to remove those below a cut-off established at four MADs (e.g. Fig. S3). Paired *t*-tests were then performed to identify statistically significan differences between the UF5 and OP4 irradiance filte treatments at each time point. Gene lists were trimmed to identify genes with fold-change differences of at least ± 2 and *P*-values ≤ 0.05. Hierarchical and k-means clustering analysis was performed with the Genesis software package (Sturn *et al*., 2002) on data from each time point, using a Euclidean squared similarity metric and data centering. Additional *k*-means analysis was performed using the EPCLUST software from the European Bioinformatics Institute (http://www.bioinf.ebc.ee/EP/EP/EPCLUST/). Genes were selected for clustering analysis if mRNA pool levels in the OP4 (VIS + UV) Cyanidiales mats deviated from that in the UF5 (VIS-only) mats by a factor of ± 2.0 (*P*-value ≤ 0.05) in at least one time point. This same selection criterion was also applied to separate analyses examining seasonal UV − VIS intensity effects. In this latter analysis, mRNA pool levels in the July 2010 VIS + UV or VIS-only algal mats needed to deviate from the January 2010 VIS + UV or VIS-only algal mats by a factor of 2.0 (*P*-value ≤ 0.05) to be included in the data set.

Microarray data have been deposited in NCBI's Gene Expression Omnibus (GEO, http://www.ncbi.nlm.nih.gov/geo/) and are accessible through the GEO Series accession number GSE37673.

Acknowledgements

Support was from the U.S. National Science Foundation (MCB 0702212) and Montana Agricultural Experiment Station (911310) to T.R.M., and from the U.S. National Science Foundation (MCB 0702177) to R.W.C. We thank Rebecca C. Mueller (University of Oregon) for assisting in the acquisition of the initial Illumina genome sequences of CCMEE 5578 and CCMEE 5508.

References

Albertano, P., Ciniglia, C., Pinto, G., and Pollio, A. (2000) The taxonomic position of *Cyanidium*, *Cyanidioschyzon*, and *Galdieria*: an update. *Hydrobiologia* **433:** 137–143.

Asimgil, H., and Kavakli, I. (2012) Purificatio and characterization of fiv members of photolyase/cryptochrome family from *Cyanidioschyzon merolae*. *Plant Sci* **185–186:** 190–198.

Brock, T.D. (1978) *Thermophilic microorganisms and life at high temperatures*. New York, NY: Springer-Verlag.

Brock, T.D., and Darland, G.K. (1970) Limits of microbial existence: temperature and pH. *Science* **169:** 1316–1318.

Ciniglia, C., Yoon, H.S., Pollio, A., Pinto, G., and Bhattacharya, D. (2004) Hidden biodiversity of the extremophilic Cyanidiales red algae. *Mol Ecol* **13:** 1827–1838.

Coesel, S., Mangogna, M., Ishikawa, T., Heijde, M., Rogato, A., *et al*. (2009) Diatom PtCPF1 is a new cryptochrome/photolyase family member with DNA repair and transcription regulation activity. *EMBO Rep* **10:** 655–661.

Ferris, M.J., Sheehan, K.B., Kuhl, M., Cooksey, K., Wiggleworth-Cooksey, B., Harvey, R., and Henson, J.M. (2005) Algal species and light microenvironment in a low-pH, geothermal microbial mat community. *Appl Environ Microbiol* **71:** 7164–7171.

Fujiwara, T., Misumi, O., Tashiro, K., Yoshida, Y., Nishida, K., Yagisawa, F., *et al*. (2009) Periodic gene expression patterns during the highly synchronized cell nucleus and organelle division cycles in the unicellular red alga *Cyanidioschyzon merolae*. *DNA Res* **16:** 59–72.

Grandbastien, M.A., Lucas, H., More, J.B., Mhiri, C., Vernhettes, S., and Casacuberta, J.M. (1997) The expression of the tobacco Tnt1 retrotransposon is linked to plant defense responses. *Genetica* **100:** 241–252.

Gross, W., and Oesterhelt, C. (1999) Ecophysiological studies on the red alga *Galdieria sulphuraria* isolated from southwest Iceland. *Plant Biol* **1:** 694–700.

Gross, W., Kuver, J., Tischendorf, G., Bouchaala, N., and Busch, W. (1998) Cryptoendolithic growth of the red alga *Galdieria sulphuraria* in volcanic areas. *Eur J Phycol* **33:** 25–31.

Gross, W., Heilmann, I., Lenze, D., and Schnarrenberger, C. (2001) Biogeography of the Cyanidiaceae (Rhodophyta) based on 18S ribosomal RNA sequence data. *Eur J Phycol* **36:** 275–280.

Huang, L., McCluskey, M.P., Ni, H., and LaRossa, R. (2002) Global gene expression profile of the cyanobacterium *Synechocystis* sp. strain PCC 6803 in response to irradiation with UV-B and white light. *J Bacteriol* **184:** 6845–6858.

Jurka, J., Kapitonov, V.V., Pavlicek, A., Klonowski, P., Kohany, O., and Walichiewicz, J. (2005) Repbase Update, a database of eukaryotic repetitive elements. *Cytogenet Genome Res* **110:** 462–467.

Kelly, D.J.A., Budd, K., and Lefebvre, D.D. (2007) Biotransformation of mercury in pH-stat cultures of eukaryotic freshwater algae. *Arch Microbiol* **187:** 45–53.

Kim, D.K., Hong, S.J., Bae, J.H., Yim, N., Jin, E.S., and Lee, C.G. (2011) Transcriptomic analysis of *Haematococcus lacustris* during astaxanthin accumulation under high irradiance and nutrient starvation. *Biotechnol Bioprocess Eng* **16:** 698–705.

Lehr, C.R., Kashyap, D.R., and McDermott, T.R. (2007a) New insights into microbial oxidation of antimony and arsenic. *Appl Environ Microbiol* **73:** 2386–2389.

Lehr, C.R., Frank, S.D., Norris, T.B., D'Imperio, S., Kalinin, A.V., Toplin, J.A., *et al*. (2007b) Cyanidia (Cyanidiales) population diversity and dynamics in an acid-sulfate-chloride spring in Yellowstone National Park. *J Phycol* **43:** 3–14.

Li, H., and Durbin, R. (2009) Fast and accurate short read alignment with burrows-wheeler transform. *Bioinformatics* **25:** 1754–1760.

Lin, C. (2000) Plant blue-light receptors. *Trends Plant Sci* **5:** 337–342.

Lin, C., and Todo, T. (2005) The cryptochromes. *Genome Biol* **6:** 220. doi:10.1186/gb-2005-6-5-220.

Lisch, D. (2002) *Mutator* transposons. *Trends Plant Sci* **7:** 498–504.

Liu, S., Yeh, C.T., Ji, T., Ying, K., Haiyan, W., Tang, H.M., *et al*. (2009) *Mu* transposon insertion sites and meiotic recombination events co-localize with epigenetic marks for open chromatin across the maize genome. *PLoS Genet* **5:** 1–13.

Long, S.P., Humphries, S., and Falkowski, P.G. (1994) Photoinhibition of photosynthesis in nature. *Annu Rev Plant Physiol Plant Mol Biol* **45:** 633–662.

Mathur, J., Bizzoco, R.W., Dean, E.G., Lipson, D.A., Poole, A.W., Levine, R., and Kelly, S.T. (2007) Effects of abiotic factors on the phylogenetic diversity of bacterial communities in acidic thermal springs. *Appl Environ Microbiol* **73:** 2612–2623.

Matsuzaki, M., Misumi, O., Shin-I, T., Maruyama, S., Takahara, M., Miyagishima, S.Y., *et al*. (2004) Genome sequence of the ultrasmall unicellular red alga *Cyanidioschyzon merolae* 10D. *Nature* **428:** 653–657.

Minoda, A., Nagasawa, K., Hanaoka, M., Horiuchi, M., Takahashi, H., and Tanaka, K. (2005) Microarray profilin of plastid gene expression in a unicellular red alga, *Cyanidioschyzon merolae*. *Plant Mol Biol* **59:** 375–385.

Minoda, A., Weber, A.P.M., Tanaka, K., and Miyagishima, S. (2010) Nucleus-independent control of the rubisco operon by the plastid-encoded transcription factor Ycf30 in the red alga *Cyanidioschyzon merolae*. *Plant Physiol* **154:** 1532–1540.

Moreno-Paz, M., Gomez, M.J., Arcas, A., and Parro, V. (2010) Environmental transcriptome analysis reveals physiological differences between biofil and planktonic modes of life of the iron oxidizing bacteria *Leptospirillum spp*. in their natural microbial community. *BMC Genomics* **11:** 404.

Nishida, K., Yagisawa, F., Kuroiwa, H., Nagata, T., and Kuroiwa, T. (2005) Cell cycle-regulated, microtubule-independent organelle division in *Cyanidioschyzon merolae*. *Mol Biol Cell* **16:** 2493–2502.

Norris, T.B., McDermott, T.R., and Castenholz, R.W. (2002) The long-term effects of UV exclusion on the microbial composition and photosynthetic competence of bacteria in hot-spring microbial mats. *FEMS Microbiol Rev* **39:** 193–209.

Nozaki, H., Takano, H., Misumi, O., Terasawa, K., Matsuzaki, M., Maruyama, S., *et al*. (2007) A 100%-complete sequence reveals unusually simple genomic features in the hot-spring red alga *Cyanidioschyzon merolae*. *BMC Biol* **5:** 28.

Oesterhelt, C., Schmalzlin, E., Schmitt, J.M., and Lokstein, H. (2007) Regulation of photosynthesis in the unicellular acidophilic red alga *Galdieria sulphuraria*. *Plant J* **50:** 500–511.

Ottesen, E.A., Marin, R., Preston, C.M., Young, C.R., Ryan, J.P., Scholin, C.A., and DeLong, E.F. (2011) Metatranscriptomic analysis of autonomously collected and preserved marine bacterioplankton. *ISME J* **5:** 1881–1895.

Park, S., Jung, G., Hwang, Y., and Jin, E. (2010) Dynamic response of the transcriptome of a psychrophilic diatom, *Chaetoceros neogracile*, to high irradiance. *Planta* **231:** 349–360.

Parro, V., Moreno-Paz, M., and González-Toril, E. (2007) Analysis of environmental transcriptomes by DNA microarrays. *Environ Microbiol* **9:** 453–464.

Pattanaik, B., Schuman, R., and Karsten, U. (2007) Effects of ultraviolet radiation on cyanobacteria and their protective mechanisms. In *Algae and Cyanobacteria in Extreme Environments*. Seckbach, J. (ed.). Dordrecht, The Netherlands: Springer, pp. 31–45.

Peddigari, S., Zhang, W., Takechi, K., Takano, H., and Takio, S. (2008) Two different clades of *copia*-like retrotransposons in the red alga *Porphyra yezoensis*. *Gene* **424:** 153–158.

Pinto, G., Ciniglia, C., Cascone, C., and Pollio, A. (2007) Species composition of Cyanidiales assemblages in Pisciarelli (Campi Flegrei, Italy) and description of *Galdieria phlegrea* sp. nov. In *Algae and Cyanobacteria in Extreme Environments*. Seckbach, J. (ed.). Dordrecht, The Netherlands.: Springer, pp. 487–502.

Poretsky, R.S., Bano, N., Buchan, A., LeCleir, G., Kleikemper, J., Pickering, M., *et al*. (2005) Analysis of

microbial gene transcripts in environmental samples. *Appl Environ Microbiol* **71:** 4121–4126.
Qin, J., Lehr, C.R., Yuan, C., Le, X.C., McDermott, T.R., and Rosen, B.P. (2009) Biotransformation of arsenic by a Yellowstone thermoacidophilic eukaryotic alga. *Proc Natl Acad Sci USA* **106:** 5213–5217.
Ramallo, E., Kalendar, R., Schulman, A.H., and Martinez-Izquierdo, J.A. (2008) *Reme1*, a *copia* retrotransposon in melon, is transcriptionally induced by UV light. *Plant Mol Biol* **66:** 137–150.
Rinta-Kanto, J.M., Bürgmann, H., Gifford, S.M., Sun, S., Sharma, S., del Valle, D.A., *et al*. (2010) Analysis of sulfur-related transcription by *Roseobacter* communities using a taxon-specifi functional gene microarray. *Environ Microbiol* **13:** 453–467.
Sagi, M., Davydov, O., Orazova, S., Yesbergenova, Z., Ophir, R., Stratmann, J.W., and Fluhr, R. (2004) Plant respiratory burst oxidase homologs impinge on wound responsiveness and development in *Lycopericon esculentum*. *Plant Cell* **16:** 616–628.
Sancar, A. (2003) Structure and function of DNA photolyase and cryptochrome blue-light photoreceptors. *Chem Rev* **103:** 2203–2237.
Schmidt, A.L., and Anderson, L.M. (2006) Repetitive DNA elements as mediators of genomic change in response to environmental cues. *Biol Rev Camb Philos Soc* **81:** 531–543.
Schroda, M., Kropat, J., Rudiger, O.W., Vallon, O., Wollman, F.A., and Beck, C.F. (2001) Possible role for molecular chaperones in assembly and repair of photosystem II. *Biochem Soc Trans* **29:** 413–418.
Senger, H. (1984) Cryptochrome: some terminological thoughts. In *Blue Light Effects in Biological Systems*. Senger, G. (ed.). The Netherlands: Springer-Verlag, pp. 72.
Shi, Y., Tyson, G.W., and DeLong, E.F. (2009) Metatranscriptomics reveals unique microbial small RNAs in the ocean's water column. *Nature* **459:** 266–269.
Skorupa, D.J., Reeb, V., Castenholz, R.W., Bhattacharya, D., and McDermott, T.R. (2013) Cyanidiales diversity in Yellowstone National Park. *Lett Appl Microbiol* **57:** 459–466.
Smith, M.W., Herfort, L., Tyrol, K., Suciu, D., Campbell, V., Crump, B.C., *et al*. (2010) Seasonal changes in bacterial and archaeal gene expression patterns across salinity gradients in the Columbia River coastal margin. *PLoS ONE* **5:** e13312. doi: 10.1371/journal.pone.0013312.
Sormacheva, I.D., and Blinov, A.G. (2011) LTR retrotransposons in plants. *Russ J Genet* **15:** 351–381.
Stewart, F.J., Sharma, A.K., Bryant, J.A., Eppley, J.M., and DeLong, E.F. (2011) Community transcriptomics reveals universal patterns of protein sequence conservation in natural microbial communities. *Genome Biol* **12:** R26.
Sturn, A., Quackenbush, J., and Trajanoski, Z. (2002) Genesis: cluster analysis of microarray data. *Bioinformatics* **18:** 207–208.
Takahashi, S., and Murata, N. (2008) How do environmental stresses accelerate photoinhibition? *Trends Plant Sci* **13:** 178–182.
Toplin, J.A., Norris, T.B., Lehr, C.R., McDermott, T.R., and Castenholz, R.W. (2008) Biogeographic and phylogenetic diversity of thermoacidophilic Cyanidiales in Yellowstone National Park, Japan, and New Zealand. *Appl Environ Microbiol* **74:** 2822–2833.
Weber, A.P., Oesterhelt, C., Gross, W., Brautigam, A., Imboden, L.A., Krassovskaya, I., *et al*. (2004) EST-analysis of the thermo-acidophilic red microalga *Galdieria sulphuraria* reveals potential for lipid A biosynthesis and unveils the pathway of carbon export from rhodoplasts. *Plant Mol Biol* **55:** 17–32.
Yokthongwattana, K., Chrost, B., Behrman, S., Casper-Lindley, C., and Melis, A. (2001) Photosystem II damage and repair cycle in the green alga, Dunaliella salina: involvement of a chloroplast-localized Hsp70. *Plant Cell Physiol* **42:** 1389–1397.
Yoon, H.S., Hackett, J.D., and Bhattacharya, D. (2002) A single origin of the peridinin- and fucoxanthin- containing plastids in the dinoflagellate through tertiary endosymbiosis. *Proc Natl Acad Sci USA* **99:** 11724–11729.
Yoon, H.S., Ciniglia, C., Wu, M., Comeron, J.M., Pinto, G., Pollio, A., and Bhattacharya, D. (2006) Establishment of endolithic populations of extremophilic Cyanidiales (Rhodophyta). *BMC Evol Biol* **6:** 78.
Zhang, W., Sakai, M., Lin, X., Takechi, K., Takano, H., and Takio, S. (2006) Reverse transcriptase-like sequences related retrotransposon in red alga, *Porphyra yezoensis*. *Biosci Biotechnol Biochem* **70:** 1999–2003.

Supporting information

Additional Supporting Information may be found in the online version of this article at the publisher's web-site:

Fig. S1. Lemonade Creek experimental site.
A. Mat with filte setups during winter. Green mat colour is typical of *Cyanidioschyzon* mats in the 37–55°C range. Pairs of UV-exposed (UV+) and UV-protected (UV–) filter for each of three biological replicates are shown as installed in the field
B. Close-up of mat illustrating effects of UV protection given by the UV filter during the summer months.
Fig. S2. Wildlife tampering with fiel equipment.
A. Grizzly bear front and rear footprints at the Lemonade Creek research site. Bar = 30 cm.
B. Bear destruction of an Igloo cooler that housed the VIS light meter and data recorder; note tooth marks.
C. Tooth and claw marks on a custom-built bear-proof container built to replace the Igloo cooler.
Fig. S3. Proportional distribution and signal strength of random control probes and gene probes. Gene probes having a signal strength below four MADs were removed and not included in the analyses described in this study. Profil is an example and illustrates the results for one of three biological replicates for UV– algal mats in April 2010.
Table S1. Summary of statistically significan UV-sensitive gene expression across four seasonal time points. Gene entries are listed so as to organize apparent UV influence separately for each of the samplings used in the microarray analyses. Only statistically significan +UV: –UV transcript levels are shown and in all cases, P-value < 0.05.
Table S2. Gene expression data for the k-means clustering analysis as a function of UV-intensity at four time points and depicted in Fig. 3. Orange color identifie a statistically

significan positive (induction) or negative (repression) expression ratio (*P*-value < 0.05).

Table S3. Summary of gene expression events linked to seasonal changes in VIS irradiance. The July : January expression ratio column denotes the statistically significan (*P*-value < 0.05) expression ratios of genes in the VIS-only mats, but which were not found to be significan in the VIS + UV algal mats.

Table S4. Summary of gene expression events inferred to be exclusively sensitive to UV wavelengths. The July : January expression ratio column denotes the statistically significan (*P*-value < 0.05) expression ratios of genes in the VIS + UV mats, but which were not found to be significan in algal protected from UV in the VIS-only mats.

Table S5. Evidence of gene expression events where both UV and VIS irradiance were influencin expression under the VIS + UV and VIS-only algal mats. The VIS + UV column denotes the statistically significan July:January expression ratio of genes in UV exposed mats, whereas the VIS-only column summarizes the statistically significan expression ratios of genes in VIS-only mats. In all cases, mRNA pool levels in the VIS-only algal mats was significantl different from VIS + UV; highlighted in orange ($P < 0.05$) or green ($P < 0.10$).